Compressive Multiplexing of Ultrasound Signals

Adrien Besson*, Dimitris Perdios*, Marcel Arditi*, Yves Wiaux†, and Jean-Philippe Thiran*‡
*Signal Processing Laboratory (LTS5), Ecole Polytechnique Fédérale de Lausanne, Lausanne, Switzerland
†Institute of Sensors, Signals, and Systems, Heriot-Watt University, Edinburgh, United-Kingdom
‡Department of Radiology, University Hospital Center (CHUV) and University of Lausanne (UNIL), Lausanne, Switzerland

***Abstract*—High-quality 3D ultrasound (US) imaging requires dense matrix-array probes with thousands of elements and necessitates an unrealistic number of coaxial cables to connect such probes to back-end systems. To address this issue, many techniques have been developed such as sparse arrays, mechanical scanning, multiplexing and micro-beamforming, which permit to achieve 3D imaging with existing 2D imaging systems but with a degradation in image quality. We propose a novel multiplexing method which relies on compressed-sensing (CS) principles to significantly reduce the number of coaxial cables. We exploit the compressive multiplexer (CMUX) introduced for radio-frequency signals to multiplex US signals in the probe head. The CMUX considers a set of signals as inputs, modulates them with chipping sequences and sums them to form a single output. On the reconstruction side, we propose two methods: one solving a CS-based problem exploiting sparsity of US signals in a pulse-stream model (CS-PS) and another one solving a least-squares problem in the Fourier domain based on bandlimited signal properties of US signals. We demonstrate through simulations and *in vivo* experiments that the proposed techniques lead to high-quality reconstruction with significantly fewer coaxial cables, up to 12× less with CS-PS.**

***Index Terms*—Compressed Sensing, multiplexing, ultrasound imaging.**

I. Introduction

HIGH-QUALITY ultrasound (US) imaging requires high-channel count matrix array probes of typically several thousands of transducer elements. Direct connection of such probes to back-end computers necessitates as many coaxial cables as the number of transducer elements, which is either unfeasible or very expensive. In order to address this issue, sparse array techniques which aim at reducing the number of receiving elements with minimal signal degradation have been investigated. Many strategies have been studied, i.e. random aperiodic layouts [1], [2] and sparse periodic layouts [3] such as vernier arrays [4] and row-column addressed arrays [5], [6]. While proposing a drastic reduction on the number of receive elements, such methods induce a significant decrease of image quality due to higher side lobes and/or grating lobes [7].

Alternative techniques have been developed including mechanical scanning based on motorized arrays [8], [9], time multiplexing [10], [11] and micro-beamforming, where an analog pre-beamforming step is performed in the probe head [12].

In this work, we propose a novel method that benefits from recent advances in modelling of US signals to allow for high-quality signal reconstructions from up to 12× fewer coaxial cables. The proposed compressive multiplexing strategy exploits the well-known compressed sensing (CS) framework. It is based on a compression module set in the probe head and a reconstruction module set in the back-end system. The compression module aims at mixing the signals in the analog domain so that they can be carried to the back-end system with fewer coaxial cables. Its main building block is the compressive multiplexer (CMUX), an analog CS architecture which has been recently introduced in the radar community [13]. The reconstruction module aims at recovering the element-raw data from compressed measurements. We implement two methods, one solving a CS-problem based on sparsity of US signals in the pulse-stream model and another one solving a least-squares problem in the frequency domain by exploiting bandlimited properties of US signals.

The remainder of the paper is organized as follows. Section II describes the proposed approach which is validated through simulations and experimental data in Section III. Concluding remarks are given in Section IV.

This work was supported in part by the UltrasoundToGo RTD project (no. 20NA21_145911) funded by Nano-Tera.ch with Swiss Confederation financing. This work was also supported by the Swiss SNF project number 205320_175974.

II. Compressive Multiplexing of Ultrasound Signals

We consider a pulse-echo US imaging configuration where a US probe, composed of N_{el} transducer elements, positioned at $(\boldsymbol{p}_i)_{i=1}^{N_{el}}$, transmits acoustic pulses and then receives backscattered echoes, as shown in Figure 1. We also consider that the medium of interest is composed of K point-reflectors positioned at $(\boldsymbol{r}_k)_{k=1}^{K}$ with a reflectivity, expressed in terms of local variations of acoustic impedance, $(\gamma(\boldsymbol{r}_k))_{k=1}^{K}$. We suppose that the reception is achieved during a time T such that the echo signal $m_i(t)$ received at the i-th element can be expressed as:

$$m_i(t) = \sum_{k=1}^{K} a_{ik} v_{pe}(t - t_{ik}), \tag{1}$$

where a_{ik} and $t_{ik} = t_{Tx}(\boldsymbol{r}_k) + t_{Rx}(\boldsymbol{r}_k, \boldsymbol{p}_i)$ are the amplitude and round-trip time of flight of the k-th point reflector seen by the i-th transducer element and $v_{pe}(t)$ is the pulse-echo waveform [14].

A. Compression Module

The main building block of the compression module is the CMUX, recently introduced in the radar community [13]. The CMUX, shown in Figure 2, takes L input signals $(m_i(t))_{i=1}^{L}$ bandlimited to B Hz, modulates each of them with chipping

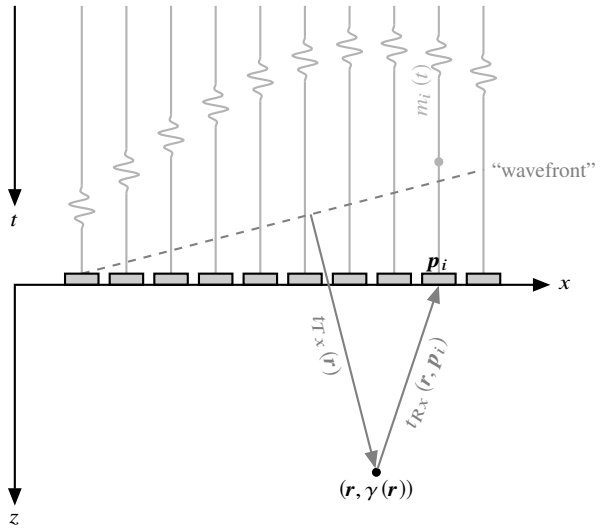

Fig. 1. Pulse-echo 2D US imaging configuration.

sequences of ± 1, $p_i(t)$, working at a rate W, and sums the modulated signals to form a single output signal $y(t)$. The analog signal is then sampled at a rate W by an analog-to-digital converter (ADC), leading to $\boldsymbol{y} \in \mathbb{R}^N$, where $N = WT$.

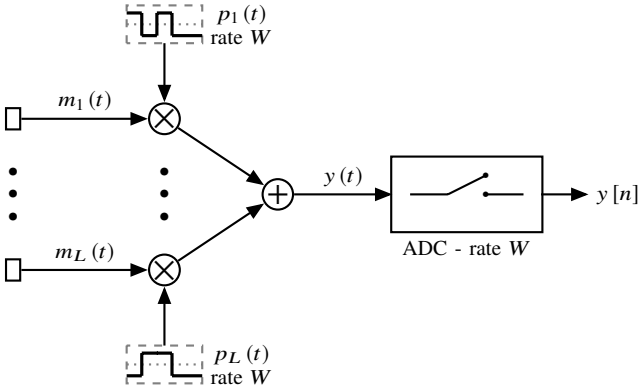

Fig. 2. Compressive multiplexer architecture.

In the CMUX architecture, the chipping sequence $p_i(t)$ spreads the spectrum of the signal $m_i(t)$ and the summation acts as an undersampling operation. If the signals $m_i(t)$ are sparse in the frequency domain, i.e. if their spectrum is composed of $S \ll LB$ non-zero frequency components, then perfect reconstruction can be achieved for a rate $W \approx S \log(LB)^q$, for $q > 1$ a small constant [13].

The proposed compression module, displayed in Figure 3, concatenates $J = N_{el}/L$ CMUXs in the probe head and outputs $\mathsf{Y} = [\boldsymbol{y}_1, \dots \boldsymbol{y}_J] \in \mathbb{R}^{N \times J}$, which are transfered to the back-end system through J cables, therefore allowing a reduction by a factor of L of the number of cables. Formally, we can write the measurement model associated with the proposed compression strategy as follows

$$\mathsf{Y} = \left(\left[\boldsymbol{p}_1, \dots, \boldsymbol{p}_{N_{el}}\right] \circ \left[\boldsymbol{m}_1, \dots, \boldsymbol{m}_{N_{el}}\right]\right) \times \mathsf{A} = (\mathsf{P} \circ \mathsf{M}) \times \mathsf{A},$$

where $\circ$ denotes the Hadamard product, $\times$ denotes the matrix product, $\mathsf{M} \in \mathbb{R}^{N \times N_{el}}$ is the raw-data sampled at rate W, $\mathsf{P} \in \mathbb{R}^{N \times N_{el}}$ is composed of the N_{el} chipping sequences and $\mathsf{A} \in \mathbb{R}^{N_{el} \times J}$ performs the summation across the elements.

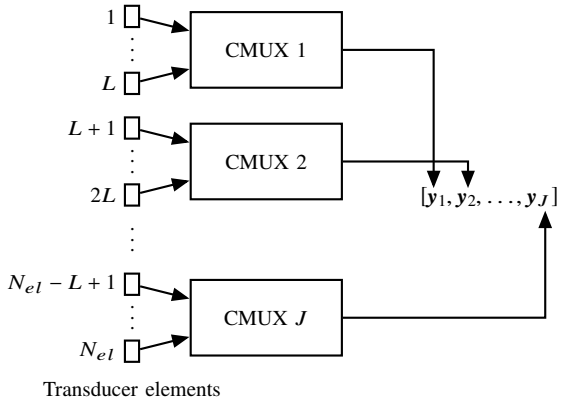

Fig. 3. Proposed compression module.

B. Reconstruction Module

The reconstruction module aims at recovering M from compressed measurements Y. We propose to exploit two well known low-dimensional models of US signals, namely the bandlimited signal model and the pulse-stream model.

The bandlimited signal model exploits the fact that the pulse-echo waveform $v_{pe}(t)$, and consequently the element raw-data, has a spectrum concentrated in a frequency band $\Xi = [f_c - F_u, f_c + F_u] \cup [-f_c - F_u, -f_c + F_u]$, where f_c is the center frequency of the transducer elements and $F_u > 0$ depends on the bandwidth of the elements. Hence, the discrete element raw-data $\boldsymbol{m}_i$, $i = 1, \dots, N_{el}$, sampled at rate W can be expressed as

$$\boldsymbol{m}_i = \mathsf{F}\hat{\boldsymbol{m}}_i + \boldsymbol{\epsilon}, \ \|\hat{\boldsymbol{m}}_i\|_0 = |J_d|,$$

where ϵ accounts for the modeling noise, $\mathsf{F} \in \mathbb{R}^{N \times N}$ is the discrete Fourier basis and $|J_d|$ is the cardinal of the following index set

$$J_d = \left\{ j \in \{1, \dots, N\} \mid W\left(-\frac{1}{2} + \frac{j-1}{N}\right) \in \Xi \right\}.$$

Hence, the vectors $\boldsymbol{m}_i$ are sparse in the frequency domain and the support J_d is usually well known such that least-squares reconstruction can be performed as follows

$$\hat{\mathsf{M}}^{\star}_{(J_d)} = \underset{\hat{\mathsf{M}} \in \mathbb{R}^{N \times N_{el}}}{\operatorname{argmin}} \left\| \mathsf{Y} - (\mathsf{P} \circ \mathsf{F}_{J_d} \hat{\mathsf{M}}_{(J_d)}) \times \mathsf{A} \right\|_F^2, \qquad (2)$$

where $\mathsf{M}_{(J_d)}$ (resp. M_{J_d}) denotes the submatrix formed by the restriction of M to the rows (resp. columns) indexed by J_d.

The pulse-stream model exploits the fact that the discretized element raw-data can be expressed using the following convolutional model

$$\boldsymbol{m}_i = \mathsf{V}_{pe}\tilde{\boldsymbol{m}}_i + \boldsymbol{\epsilon}', \ \|\tilde{\boldsymbol{m}}_i\|_0 \leq K,$$

where $\mathsf{V}_{pe} \in \mathbb{R}^{N \times N}$ is a convolutional dictionary made of shifted replica of the discretized pulse-echo waveform, $\tilde{\boldsymbol{m}}_i \in$

$\mathbb{R}^N$ and $\boldsymbol{\epsilon}' \in \mathbb{R}^N$ accounts for modelling and measurement noise. We reconstruct the element-raw data by solving the following synthesis problem

$$\mathsf{M}^\star \in \mathsf{V}_{pe} \underset{\tilde{\mathsf{M}} \in \mathbb{R}^{N \times N_{el}}}{\operatorname{argmin}} \left\| \mathsf{Y} - (\mathsf{P} \circ \mathsf{V}_{pe} \tilde{\mathsf{M}}) \times \mathsf{A} \right\|_F^2 + \sum_{i=1}^{N_{el}} \lambda_i \left\| \tilde{\mathsf{M}}_i \right\|_1, \quad (3)$$

where $\lambda_i \in \mathbb{R}_+$, $i = 1, \ldots, N_{el}$ are the regularization parameters. By several reshaping operations, (3) can be recast as a standard weighted ℓ_1-minimization problem which can be solved using the fast iterative shrinkage thresholding algorithm (FISTA) [15]. In the remainder of the paper, the reconstruction method using the bandlimited signal model described above is denoted as LS-F and the one based on the pulse-stream model as CS-PS.

III. Experiments and Results

A. Simulated PICMUS Phantom

A first experiment is performed within the framework of the PICMUS challenge [16], whose details are available on the dedicated website[1]. We work on the numerical phantom and simulate two compression strategies: one based on 8 input signals per CMUX working at a rate of 62.5 MHz, achieving a compression of 8× on the number of coaxial cables, and one based on 4 input signals per CMUX working at 31.25 MHz, achieving a compression of 4× on the number of coaxial cables We simulate a single PW insonification with normal incidence. The impulse response is a Gaussian modulated sinusoidal pulse, centered at 5 MHz with 60 % bandwidth, and the excitation is a 1-cycle square signal. The chipping sequences are generated as random sequence of ±1.

Regarding the CS-PS reconstruction strategy, we manually set the regularization parameters, we fix a maximum of 1000 iterations and a stopping criterion based on the relative evolution of the solution. Regarding LS-F, the least-squares problem is solved with the well known LSQR method with a maximum number of iterations of 2000 and a stopping criterion based on a tolerance of 1×10^{-8} on the residual.

Once the element raw-data are reconstructed from compressed measurements, we obtain a radio-frequency (RF) image by performing delay-and-sum beamforming with spline interpolation and with apodization coefficients taking into account element directivity. Standard post-processing is performed on the RF image, i.e. envelope detection, normalization and log-compression for display.

We evaluate the reconstruction methods based on several metrics defined in the context of the challenge[2], i.e. contrast-to-noise ratio (CNR), average lateral and axial resolutions at 14 mm and 45 mm and speckle test (number of regions that pass the test).

[1] https://www.creatis.insa-lyon.fr/EvaluationPlatform/picmus/about.html

[2] https://www.creatis.insa-lyon.fr/EvaluationPlatform/picmus/about_speckle_quality.html

The results, reported in Table I, show that the images reconstructed with the proposed strategies exhibit qualities similar to the reference image obtained without compression.

TABLE I
Comparison of the Methods on the Numerical PICMUS Phantom

Method	Freq.	CNR [dB]	Lat. Res. [mm] 14 mm	Lat. Res. [mm] 45 mm	Ax. Res. [mm] 14 mm	Ax. Res. [mm] 45 mm	Speck.
LS-F		5.90	0.33	0.51	0.38	0.42	6/6
CS-PS	62.5	6.10	0.33	0.51	0.38	0.42	6/6
Reference		5.90	0.33	0.51	0.37	0.40	6/6
LS-F		5.90	0.33	0.51	0.38	0.41	4/6
CS-PS	31.25	6.40	0.34	0.52	0.38	0.41	6/6
Reference		5.90	0.33	0.51	0.37	0.40	6/6

B. Sequence of In Vivo Carotids

We acquire two 0.5 s-long sequences (approx. 40 frames) of *in vivo* carotids, one longitudinal and one cross-section, with a Verasonics Vantage 256™ (Verasonics, WA, USA) equipped with a GE 9L-D probe (linear array, 192 elements, 5.2 MHz center frequency, 75 % bandwidth). We transmit a single plane wave with normal incidence with 3-cycle square excitation signal. We acquire the data at 62.5 MHz and we simulate two CMUX compression strategies, one with 8 input signals per CMUX and one with 12 input signals per CMUX, resulting in a compression equivalent to 8× and 12× on the number of coaxial cables, respectively.

We use the same settings as for the simulated experiment for the reconstruction methods, beamforming and post-processing. Regarding CS-PS, we approximate the impulse response of the transducer elements by a Gaussian modulated sinusoidal pulse. To quantify the image quality, the average peak-signal-to-noise-ratio (PSNR) and structural similarity index (SSIM) are computed against the reference sequence reconstructed from data that have not been compressed.

Table II reports the values of SSIM and PSNR for LS-F and CS-PS for the two considered compression strategies. We observe that both methods lead to high-quality reconstruction for a compression ratio of 8, with slightly better results for LS-F. This may be explained by the imperfect knowledge of the pulse shape which impacts the quality of the reconstruction with CS-PS. Regarding the reconstruction with a compression ratio of 12, we observe that CS-PS significantly outperforms LS-F, which can be explained by a potentially sparser representation of US signals in the pulse stream model than with the bandlimited signal model, especially when the bandwidth is relatively high.

Figure 4 displays the log-compressed B-mode images of a single frame of the sequence of longitudinal carotids for the compression ratio of 8. Visual assessment of the images corroborates the above analysis of the metrics and shows the remarkable quality of the reconstruction with the proposed approaches.

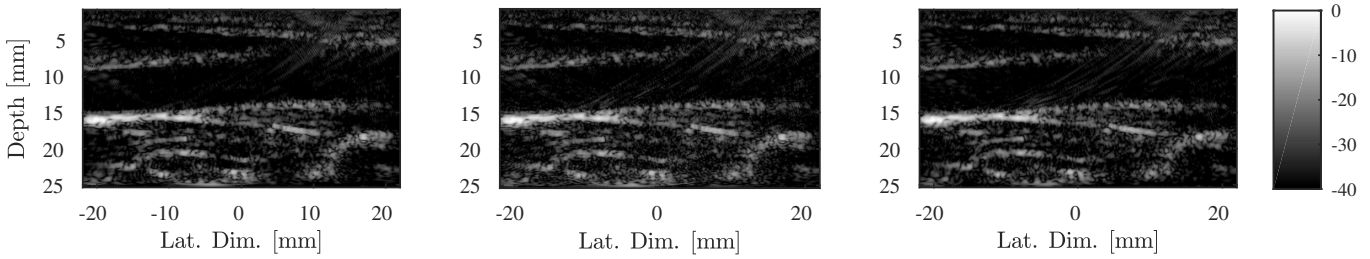

Fig. 4. From left to right: reference log-compressed B-mode image (40 dB dynamic range); log-compressed B-mode image reconstructed with LS-F (compression ratio of 8); log-compressed B-mode image reconstructed with CS-PS (compression ratio of 8).

TABLE II
COMPARISON OF THE METHODS ON THE IN VIVO CAROTID

Method	Acquisition	Compression Ratio [–]	PSNR [dB]	SSIM [–]
LS-F	Longitudinal	8	44.5	0.96
CS-PS			42.2	0.96
LS-F		12	33.2	0.79
CS-PS			38.7	0.91
LS-F	Cross-section	8	42.6	0.95
CS-PS			40.3	0.95
LS-F		12	34.3	0.82
CS-PS			37.1	0.90

IV. CONCLUSION

We propose a compressive multiplexing approach for ultrasound signals which aims at reducing the number of coaxial cables to connect the probe to the back-end computer. The compression module, that would be located in the head of the probe, is composed of several compressive multiplexers (CMUX). Each CMUX takes few input signals, modulates each of them with a chipping sequence and sums them to output a single signal. The reconstruction module, that would be located in the back-end computer, reconstructs the element raw data from the compressed measurements. We suggest two reconstruction methods, one solving a least-square problem in the Fourier domain, based on the bandlimited signal property of the element raw data, and one solving a CS problem based sparsity on the pulse-stream model. We demonstrate through simulations and *in vivo* experiments that the proposed technique may lead to high-quality reconstruction with up to 12× fewer coaxial cables. The proposed method, combined with existing approaches, e.g. sparse array techniques, may allow to perform 3D imaging with significantly fewer elements than any existing method.

REFERENCES

[1] D. Turnbull and F. Foster, "Beam steering with pulsed two-dimensional transducer arrays," *IEEE Trans. Ultrason. Ferroelectr. Freq. Control*, vol. 38, no. 4, pp. 320–333, 1991.

[2] A. Trucco and V. Murino, "Stochastic optimization of linear sparse arrays," *IEEE J. Ocean. Eng.*, vol. 24, no. 3, pp. 291–299, 1999.

[3] S. Smith, H. Pavy, and O. von Ramm, "High-speed ultrasound volumetric imaging system. I. Transducer design and beam steering," *IEEE Trans. Ultrason. Ferroelectr. Freq. Control*, vol. 38, no. 2, pp. 100–108, 1991.

[4] G. Lookwood and F. Foster, "Optimizing the radiation pattern of sparse periodic two-dimensional arrays," *IEEE Trans. Ultrason. Ferroelectr. Freq. Control*, vol. 43, no. 1, pp. 15–19, 1996.

[5] C. Morton and G. Lockwood, "Theoretical assessment of a crossed electrode 2-D array for 3-D imaging," in *IEEE Symp. Ultrason. 2003*, 2003, pp. 968–971.

[6] C. H. Seo and J. T. Yen, "A 256 × 256 2-D array transducer with row-column addressing for 3-D rectilinear imaging," *IEEE Trans. Ultrason. Ferroelectr. Freq. Control*, vol. 56, no. 4, pp. 837–847, 2009.

[7] J. Yen, J. Steinberg, and S. Smith, "Sparse 2-D array design for real time rectilinear volumetric imaging," *IEEE Trans. Ultrason. Ferroelectr. Freq. Control*, vol. 47, no. 1, pp. 93–110, 2000.

[8] S. W. Hughes, T. J. D'Arcy, D. J. Maxwell, W. Chiu, A. Milner, J. E. Saunders, and R. J. Sheppard, "Volume estimation from multiplanar 2D ultrasound images using a remote electromagnetic position and orientation sensor," *Ultrasound Med. Biol.*, vol. 22, no. 5, pp. 561–572, 1996.

[9] J. M. Griffith and W. L. Henry, "A sector scanner for real time two-dimensional echocardiography," *Circulation*, vol. 49, no. 6, pp. 1147–1152, 1974.

[10] J. T. Yen and S. W. Smith, "Real-time rectilinear 3-D ultrasound using receive mode multiplexing," *IEEE Trans. Ultrason. Ferroelectr. Freq. Control*, vol. 51, no. 2, pp. 216–226, 2004.

[11] J. S. Kenji Hara, "A new 80V 32x32ch low loss multiplexer LSI for a 3D ultrasound imaging system," in *Proceedings. ISPSD '05. 17th Int. Symp. Power Semicond. Devices ICs, 2005.* IEEE, 2005, pp. 359–362.

[12] B. Savord and R. Solomon, "Fully sampled matrix transducer for real time 3D ultrasonic imaging," in *IEEE Symp. Ultrason. 2003*, vol. 1, 2003, pp. 945–953.

[13] J. P. Slavinsky, J. N. Laska, M. a. Davenport, and R. G. Baraniuk, "The compressive multiplexer for multi-channel compressive sensing," in *2011 IEEE Int. Conf. Acoust. Speech Signal Process.*, no. 3, 2011, pp. 3980–3983.

[14] J. A. Jensen and N. B. Svendsen, "Calculation of pressure fields from arbitrarily shaped, apodized, and excited ultrasound transducers," *IEEE Trans. Ultrason. Ferroelectr. Freq. Control*, vol. 39, no. 2, pp. 262–267, 1992.

[15] A. Beck and M. Teboulle, "A fast iterative shrinkage-thresholding algorithm for linear inverse problems," *SIAM J. Imaging Sci.*, vol. 2, no. 1, pp. 183–202, 2009.

[16] H. Liebgott, A. Rodriguez-Molares, F. Cervenansky, J. Jensen, and O. Bernard, "Plane-wave imaging challenge in medical ultrasound," in *2016 IEEE Int. Ultrason. Symp.*, sep 2016.